

Estimating IF shifts based on SU(1,1) interferometer

Yuetao Chen¹, Gaiqing Chen¹, Mengmeng Luo², Shoukang Chang^{1,*} and Shaoyan Gao^{1†}

¹MOE Key Laboratory for Nonequilibrium Synthesis and Modulation of Condensed Matter,

Shaanxi Province Key Laboratory of Quantum Information and Quantum Optoelectronic Devices,
School of Physics, Xi'an Jiaotong University, 710049, People's Republic of China

²Department of Physics, Xi'an Jiaotong University City College, Xi'an 710018, China

IF (Imbert–Fedorov) shifts which refers to a transverse micro-displacement occurs at the interface between two media. The estimation of such micro-displacement enables a deeper understanding of light-matter interactions. In this paper, we propose a theoretical scheme to investigate the IF shifts and incident angle sensitivity by introducing SPR sensor into the SU(1,1) interferometer. By injecting two coherent states in the SU(1,1) interferometer, we obtain the sensitivity of the IF shifts and incident angle based on the homodyne detection. Our results demonstrate that it is possible to get the maximal IF shift and the optimal IF shifts sensitivity simultaneously. Meanwhile, the orbit angular momentum carried by Laguerre-Gauss (LG) beam is unfavorable for improving the IF shift sensitivity. Furthermore, we have investigated the sensitivity of the incident angle in our scheme and found that it is capable of surpassing the sensitivity limit of $(6 \times 10^{-6})^\circ$. This allows us to achieve a more precise IF shifts sensitivity than the traditional weak measurement method used for IF shift detection, which typically has a rotation precision limit of 0.04° [Journal of Optics, 19(10), 105611]. More importantly, both the sensitivity of IF shifts and incident angle can breakthrough the (shot noise limit) SNL, even approaching the Cramér-Rao bound (QCRB) at the incident angle $\theta = 43.6208^\circ$ and $\theta = 43.6407^\circ$. We also discover that increasing the coherent amplitude is beneficial for improving the sensitivity of both the IF shifts and incident angle. Our findings shall offer a novel scheme for measuring micro-displacement in SPR sensor. These results can be helpful in the development of more precise quantum-based sensors for studying light-matter interactions.

PACS: 03.67.-a, 05.30.-d, 42.50.Dv, 03.65.Wj

I. INTRODUCTION

Quantum metrology has attracted wide attention since it can achieve ultra-high precision estimation of various physical quantities by using some quantum effects, such as squeezing, nonclassicality and entanglement, and therefore has a lot of applications in many other fields, including gravitational wave detection [7, 8], quantum imaging [9–11] and quantum thermometry [12–14]. As one of the important platforms to realize quantum metrology, optical interferometer has attracted extensive attention in recent years. Accordingly, various optical interferometers have been proposed to realize the precise measurement of many physical quantities, such as phase shift, angular displacement and field-quadrature displacement. At the beginning of quantum metrology, one mainly injects some non-classical quantum states into the traditional Mach–Zehnder interferometer (MZI) to enhance the phase or angular displacement sensitivity. In particular, Caves proposed a feasible scheme, that is, using squeezed vacuum state instead of coherent state to significantly improve the phase sensitivity of MZI. Since then, non-classical quantum states, involving twin Fock states, NOON state and two-mode squeezed vacuum state, are used for achieving higher phase shift or angular displacement precision, even beating the Heisen-

berg limit (HL). Although using non-classical states can realize the improvement of phase or angular displacement sensitivity of the optical interferometer, these quantum states are not only difficult to generate by using existing experimental techniques, but also very vulnerable to the impact of noise environment. Hence one began to pay attention to whether the devices of optical interferometer can enhance the measurement accuracy. For instance, Yurke *et al.* suggested for the first time to replace two linear optical beam splitters of the conventional MZI with nonlinear optical parametric amplifiers, thus putting forward the SU(1,1) interferometer and further showed that the phase sensitivity of the SU(1,1) interferometer can break through the shot noise limit (SNL). In recent decades, many theoretical and experimental schemes based on the SU(1,1) interferometer have been proposed extensively. One of these schemes was given by Li *et al.*, who theoretically demonstrated that the SU(1,1) interferometer based on the homodyne detection can realize the HL sensitivity by using a coherent state and a squeezed vacuum state as input states. Subsequently, Liu *et al.* showed that the SNL of the angular displacement can be surpassed by using a coherent state as the input state of the SU(1,1) interferometer.

In addition to the phase estimation, angular displacement estimation and field-quadrature displacement estimation, the quantum sensor based on the Kretschmann structure has attracted wide attention in experiment and theory. Especially, the two types of nonlinear interferometric surface-plasmon-resonance sensor proposed by Wang *et al.*, in which Kretschmann structure is placed inside or outside SU(1,1) interferometer [43]. We also no-

*Corresponding author. changshoukang@stu.xjtu.edu.cn

†Corresponding author. gaosy@xjtu.edu.cn

ticed that the Imbert–Fedorov (IF) shift estimation and incident angle estimation has not been studied yet based on the SU(1,1) interferometer. It is well known that when a bounded light beam is illuminated to an interface of two different medium, the reflected light beam will experience transverse shifts which are called IF shifts [26]. IF shifts depend sensitively on the refractive index of the medium. In other words, the information of refractive index of the medium can be discerned by observing the variation in IF shifts. Thus, IF shifts attract renewed attention in various field such as optical sensors [27], precision metrology and nanophotonic devices [28–30]. Generally, large IF shifts can be obtained in the surface plasmon resonance (SPR) sensors and measured in weak measurement scheme. However, there are always existing error in SPR sensors which will lead to low precision in the measurement of IF shifts. Besides, in recent decades, it is found that no matter how to improve the traditional measurement scheme by using traditional means, the measurement accuracy can not be substantially improved owing to the existence of classical noise. The precision limit constrained by classical noise is known as the shot-noise limit (also known as the standard quantum limit) [31, 32]. As described above, the SU(1,1) interferometer which is an important tool for the precision measurement could also be good candidates for the IF shifts measurement. Thus, in this paper, we theoretically investigate the IF shift sensitivity for a Laguerre Gaussian reflected beam in a surface plasmon resonance sensor via the SU(1,1) interferometer. By taking the homodyne detection at one of output ports of the SU(1,1) interferometer, we obtain the IF shift and incident angle sensitivity. Then, the SNL and the quantum Cramér-Rao bound (QCRB) are also analytically derived. The numerical results show that the sensitivity of IF shifts and incident angle can surpass the SNL, even approaching the QCRB around the SPR angle. Moreover, the maximal IF shifts and the minimum IF shifts sensitivity can be obtained simultaneously. The incident angle sensitivity can break through $(6 \times 10^{-6})^\circ$ which shows more accurate compared with the rotation precision of 0.04° in the weak measurement of IF shifts [34].

The paper is organized as follows. In Sec. II, we present a description of the Kretschmann structure and IF shifts. In Sec. III, we describe the interaction process between incident coherent beam and the SPR sensors in nonlinear transmissivity estimation model. In Sec. IV, the sensitivity of IF shifts and incident angle is investigated via homodyne detection. In Sec. V, we obtain the QCRB and SNL of IF shifts and incident angle and compare them with the sensitivity of IF shifts and incident angle. Finally, the main conclusions are presented in the last section.

II. KRETSCHMANN STRUCTURE AND IMBERT–FEDOROV SHIFTS

For the sake of facilitating the discussion of the Imbert–Fedorov shift estimation based on the SU(1,1) interferometer, we briefly review the known results of the Kretschmann structure and the Imbert–Fedorov (IF) shifts in this section. As shown in Fig. 1, the Laguerre–Gaussian beam is illuminated to the Kretschmann structure which consists of three layers, the top layer is a prism, the middle is a thin gold film coated on prism which leads to surface plasmon resonance and the bottom is semi-infinite vacuum. The global coordinate system is marked as $(x_g; y_g; z_g)$, while the local coordinate systems are represented by $(x_i; y_i; z_i)$ and $(x_r; y_r; z_r)$ which are attached to the incident and reflected beams, respectively. Assume that a TM-polarized Laguerre-Gauss beam is incident onto the Au film from the glass prism, after reflection there will be IF shifts in the y_g direction at the glass-Au interface. The angular spectrum of the incident TM-polarized Laguerre-Gauss beam can be represented by

$$\tilde{E}_i = [w_0(-ik_{ix} + \text{sgn}[l])k_{iy}/\sqrt{2}]^{|l|} e^{-(k_{ix}^2 + k_{iy}^2)w_0^2/4}, \quad (1)$$

where l and $k_{i\lambda}$ ($\lambda = x, y$) is the units of orbit angular momentum and the lateral wave vectors of incident beam, respectively, the beam waist w_0 is $1000\mu\text{m}$, the symbolic function $\text{sgn}[l]$ can be defined by

$$\text{sgn}[l] = \begin{cases} 1, l > 0 \\ 0, l = 0 \\ -1, l < 0 \end{cases}. \quad (2)$$

The Imbert–Fedorov shifts are related to the complex reflection coefficient r_{pgv} of the Kretschmann configuration given by

$$r_{pgv} = \frac{r_{pg} + r_{gv}e^{2ik_gz_d}}{1 + r_{pg}r_{gv}e^{2ik_gz_d}}, \quad (3)$$

where d denotes the thickness of gold film and the reflection coefficient between the n th and m th layers r_{nm} can be expressed as

$$r_{nm} = \frac{k_{nz}\varepsilon_m - k_{mz}\varepsilon_n}{k_{nz}\varepsilon_m + k_{mz}\varepsilon_n}, \quad (4)$$

where $n, m = (\text{p}(\text{prism}), \text{g}(\text{gold}), \text{and } \text{v}(\text{vacuum}))$, and k_{nz} represents the normal component of the wave vector in the n th layer and can be given by

$$\begin{aligned} k_{nz} &= \frac{2\pi}{\lambda} \sqrt{\varepsilon_n - \varepsilon_p(\sin\theta)^2}, \\ k_{mz} &= \frac{2\pi}{\lambda} \sqrt{\varepsilon_m - \varepsilon_p(\sin\theta)^2}, \end{aligned} \quad (5)$$

where θ is the incident angle, ε_p and ε_g are the permittivities of prism and gold film, respectively, λ is the wavelength of incident light of TM-polarized Laguerre-Gauss

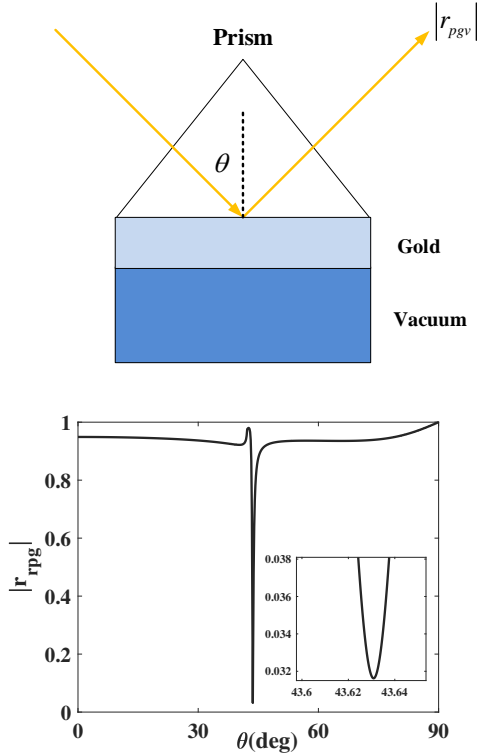


FIG. 1: (Color online) (a) An attenuated total reflection for Laguerre–Gaussian beam in the SPR sensor. (b) Reflectivity $|r_{pgv}|$ of Kretschmann structure as a function of the incident angle.

beam. For simplicity, we choose the gold film with the thickness $d = 47nm$, the prism and vacuum are semi-infinite. In order to visually see what the value of the incident angle takes, a large IF shifts can be generated. At fixed values of $\epsilon_p = 2.22$, $\epsilon_g = -20.327 + 1.862i$, $d = 47nm$ and $\lambda = 780nm$, we plot the reflectivity $|r_{pgv}|$ of Kretschmann structure as a function of the incident angle as shown in Fig. 1(b). It is clear that the reflectivity $|r_{pgv}|$ can reach the minimum value at the incident angle $\theta = 43.63^\circ$, and this incident angle is also called the SPR angle. The reason for this phenomenon is that the excitation of surface plasmon modes and reflectivity is dramatically attenuated at this incident angle. The sharp variation in reflectivity near the SPR angle will give rise to huge IF shifts and the shifts can be simplified as follow in the condition of large w_0 [35].

$$Y = -l \frac{\partial |r_{pgv}| / \partial \theta}{k_0 |r_{pgv}|}, \quad (6)$$

where k_0 is wave vector of incident light in vacuum.

In Fig. 2, we plot the Y/λ as a function of the incident angle, when given parameters $\epsilon_p = 2.22$, $\epsilon_g = -20.327 + 1.862i$, $d = 47nm$ and $\lambda = 780nm$. According to Eq. (6), Y varies with $(\partial |r_{pgv}| / \partial \theta) / |r_{pgv}|$, therefore

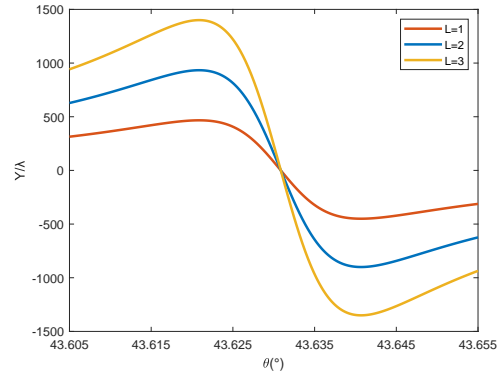


FIG. 2: (Color online) IF shifts as a function of the incident angle θ with $L = 1$, $L = 2$ and $L = 3$.

Y can be enhanced when the SPR is excited. At the SPR angle, $Y = 0$ since $\partial |r_{pgv}| / \partial \theta = 0$. When the incident angle cross the SPR angle, the value of Y changes from positive to negative, as $\partial |r_{pgv}| / \partial \theta$ changes sign. Thus, a positive peak and a negative peak can be found in Fig. 2, which locate at $\theta = 43.6208^\circ$ and $\theta = 43.6407^\circ$, respectively. For different incident OAM l , these two kinds of peaks can always be existing, as shown by Fig. 2. As OAM l increase, IF shifts will be amplified linearly with it according to Eq. (6) and the peak positions are always located at the SPR angle. The maximum shifts for the cases of $l = \pm 3$ are $1092\mu m$. Thus, huge IF shifts can be obtained in Kretschmann structure with Laguerre–Gaussian incident beam. This also means that we are able to capture the properties of medium such as excitation of surface plasmon modes from IF shifts. However, there always exist error in IF displacement due to the limitation of incident angle accuracy. Therefore, we need device to get accurate measurement of displacement.

III. NONLINEAR TRANSMISSIVITY ESTIMATION MODEL

The fundamental condition of the IF shift have been discussed in the previous section, in what follows, we will introduce the IF shifts sensors via the SU(1,1) interferometer. As shown in Fig. 3, we consider two coherent states $|\alpha\rangle_a \otimes |\beta\rangle_b$ with $z = |z| e^{i\theta_z}$, $z = \alpha, \beta$ as the inputs in mode a and mode b , respectively. After going through the first OPA, mode b is regarded as a reference beam, while mode a enters the Kretschmann structure to generate the IF shift to be estimated. The action of the first OPA on two coherent states $|\alpha\rangle_a \otimes |\beta\rangle_b$ can be described by the unitary operator $\hat{S}(\xi_1) = \exp(\xi_1^* \hat{a} \hat{b} - \xi_1 \hat{a}^\dagger \hat{b}^\dagger)$, $\xi_1 = g_1 e^{i\theta_1}$. The interaction process between mode a and the Kretschmann structure can be simulated by the fictitious beam splitter $\hat{U}_{BS} = \exp[(\hat{a}^\dagger \hat{a}_v - \hat{a} \hat{a}_v^\dagger) \arctan \sqrt{(1-\eta)/\eta}]$ with the transmissivity $\eta = |r_{pgv}|^2$, which can be achieved experimentally by inserting the variable neutral

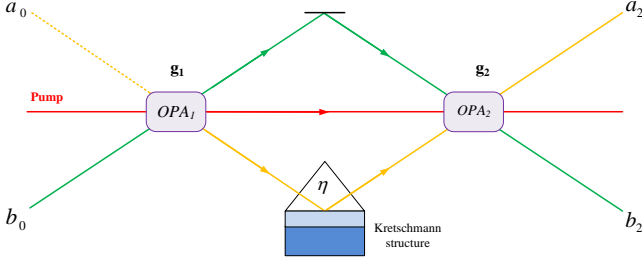


FIG. 3: (Color online) Schematic diagram of SU(1,1) interferometer with SPR sensors. The two input ports of this interferometer are a coherent state $|\alpha\rangle_a$ and a vacuum state $|\beta\rangle_b$

density filter in the optical path a [36]. Then, the modes a and b recombine in the second OPA. Let \hat{a} (\hat{a}^\dagger) and \hat{b} (\hat{b}^\dagger) are the annihilation (creation) operators for the modes a and b , respectively. Then, the relation between the output operators \hat{a}_2 and \hat{b}_2 and the input operators \hat{a}_0 and \hat{b}_0 can be expressed as

$$\begin{aligned}\hat{a}_2 &= W_1\hat{a}_0 - W_2\hat{b}_0^\dagger + W_3\hat{a}_v, \\ \hat{b}_2 &= W_4\hat{b}_0 - W_5\hat{a}_0^\dagger + W_6\hat{a}_v^\dagger,\end{aligned}\quad (7)$$

where

$$\begin{aligned}W_1 &= \sqrt{\eta} \cosh g_1 \cosh g_2 + e^{i(\theta_2 - \theta_1)} \sinh g_1 \sinh g_2, \\ W_2 &= \sqrt{\eta} e^{i\theta_1} \sinh g_1 \cosh g_2 + e^{i\theta_2} \cosh g_1 \sinh g_2, \\ W_3 &= \sqrt{1 - \eta} \cosh g_2, \\ W_4 &= \cosh g_1 \cosh g_2 + \sqrt{\eta} e^{i(\theta_2 - \theta_1)} \sinh g_1 \sinh g_2, \\ W_5 &= e^{i\theta_1} \sinh g_1 \cosh g_2 + \sqrt{\eta} e^{i\theta_2} \cosh g_1 \sinh g_2, \\ W_6 &= -\sqrt{1 - \eta} e^{i\theta_2} \sinh g_2,\end{aligned}\quad (8)$$

where g_j and θ_j ($j = 1, 2$) are the gain factor and phase shift of OPA $_j$ process, respectively, and \hat{a}_v correspond to the input vacuum field associated with the introduction of the fictitious beam splitter [36].

IV. IF SHIFTS SENSITIVITY VIA HOMODYNE DETECTION

In this section, we mainly investigate the IF shift sensitivity based on the SPR sensor. To this end, we need to choose a specific detection method for reading the IF shift information at the final output port. In fact, there are many distinct types of detecting methods, such as homodyne detection [24], intensity detection [37–39], and parity detection [40–42]. Moreover, compared with the intensity detection and parity detection, homodyne detection is easily achieved using existing experimental technology. Therefore, we use the homodyne detection to estimate the IF shift, the corresponding detected variable is the amplitude quadrature \hat{X} , i.e.,

$$\hat{X} = \frac{\hat{a}_2 + \hat{a}_2^\dagger}{\sqrt{2}}. \quad (9)$$

For the sake of discussion, we consider the balanced situation between two OPAs processes, i.e., $\theta_2 - \theta_1 = \pi$, and $g_1 = g_2 = g$ (let $\theta_1 = 0$ for simplicity) in the following. According to the error propagation formula, the IF shift sensitivity can be given by

$$\begin{aligned}\Delta Y &= \frac{\sqrt{\Delta^2 \hat{X}}}{\left| \partial \langle \hat{X} \rangle / \partial Y \right|}, \\ &= \frac{\sqrt{\Delta^2 \hat{X}}}{\left| (\partial \langle \hat{X} \rangle / \partial \eta) (\partial \eta / \partial Y) \right|},\end{aligned}\quad (10)$$

where

$$\begin{aligned}\Delta^2 \hat{X} &= \langle \hat{X}^2 \rangle - \langle \hat{X} \rangle^2 \\ &= \frac{1}{2} [(\sqrt{\eta} \cosh^2 g - \sinh^2 g)^2 \\ &\quad + (\sqrt{\eta} - 1)^2 \sinh^2 g \cosh^2 g \\ &\quad + (1 - \eta) \cosh^2 g], \\ \langle \hat{X} \rangle &= \sqrt{2} [|\alpha| (\sqrt{\eta} \cosh^2 g - \sinh^2 g) \cos \theta_\alpha \\ &\quad - |\beta| (\sqrt{\eta} - 1) \sinh g \cosh g \cos \theta_\beta], \\ Y &= -l \frac{\partial \eta / \partial \theta}{k_0 \eta}.\end{aligned}\quad (11)$$

In Fig. 4(a), we show IF shifts Y changing with θ for Laguerre Gaussian reflected beam when given parameters $g = 0.7$, $\theta_\alpha = 0$, $\theta_\beta = \pi$, $L = 1$, and $|\alpha| = |\beta| = 50000$. We can clearly see that there is a positive and negative peaks of IF shifts which is located at $\theta = 43.6208^\circ$ and $\theta = 43.6407^\circ$ on two sides of the SPR angle and IF shifts vanish at the SPR angle ($\theta = 43.6309^\circ$). The corresponding IF shifts sensitivity ΔY as a function of θ is shown in Fig. 4(b). It is clearly seen that IF shifts sensitivity ΔY experiences sharp variations at two dips located at $\theta = 43.6208^\circ$ and $\theta = 43.6407^\circ$ on two sides of SPR angle and the minimum value of the IF shifts sensitivity can be achieved at $\theta = 43.6208^\circ$ and $\theta = 43.6407^\circ$. This implies that large IF shifts and small IF shifts sensitivity can be obtained simultaneously. Further, to show how the IF shifts sensitivity is affected by the coherence amplitude $|\alpha|$ and $|\beta|$, at $\theta = 43.6208^\circ$ and $\theta = 43.6407^\circ$, we also plot the IF shifts sensitivity as a function of $|\alpha|$ and $|\beta|$ in Fig. 5(a) and 5(b), respectively. It can be found that, IF shifts sensitivity ΔY decrease sharply with the increase of $|\alpha|$ and $|\beta|$, for the case of $\theta = 43.6208^\circ$ and $\theta = 43.6407^\circ$.

Moreover, the effect of the orbital angular momentum on IF shifts sensitivity is also shown in Fig. 6 with different L changing with θ when other parameters are the

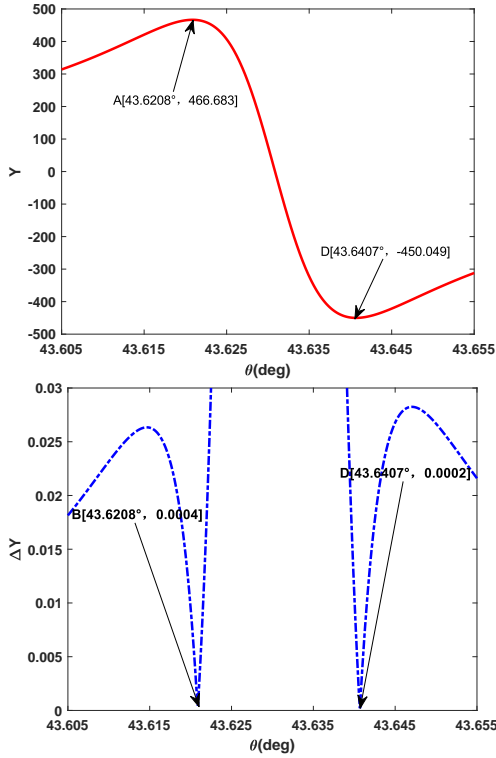


FIG. 4: (a) IF shifts in SPR sensors, (b) IF shifts sensitivity based on homodyne detection as a function of θ with $g = 0.7$, $\theta_\alpha = 0$, $\theta_\beta = \pi$, $L = 1$, and $|\alpha| = |\beta| = 50000$. The blue-dashed line and the black-solid line correspond to IF shifts sensitivity (ΔY) and IF shifts (Y), respectively.

same as those in Fig. 4. It is obviously that the minimum value of the IF shifts sensitivity can still be obtained at the same point $\theta = 43.6208^\circ$ and $\theta = 43.6407^\circ$ with different L , and the IF shifts sensitivity increases linearly with L . Thus, we conclude that large IF shifts and small IF shifts sensitivity can be obtained at $\theta = 43.6208^\circ$ and $\theta = 43.6407^\circ$ simultaneously with different L .

V. INCIDENT ANGLE SENSITIVITY VIA HOMODYNE DETECTION

In the previous section, we have discussed the IF shifts sensitivity based on the homodyne detection. It's worth noting that the IF shifts can be observed in the weak measurement scheme [34]. Moreover, the rotation of the polarizer in the weak measurement scheme [34] will lead to the error of incident angle which is the main cause of the error of IF shifts (ΔY). For this reason, we further need to investigate the incident angle sensitivity. In a similar way to obtain the IF shift sensitivity in section 4, one can also derive the incident angle sensitivity

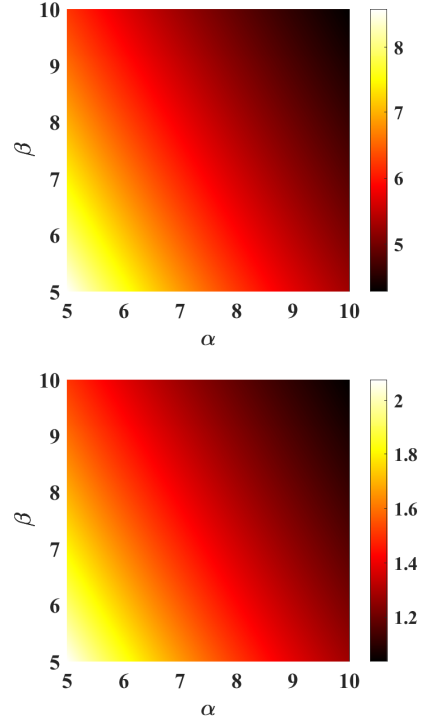


FIG. 5: (Color online) IF shifts sensitivity based on homodyne detection as a function of the coherent amplitude $|\alpha|$ and $|\beta|$ with $g = 0.7$, $\theta_\alpha = 0$, $\theta_\beta = \pi$ and $L = 1$ at (a) $\theta = 43.6208^\circ$, and (b) $\theta = 43.6407^\circ$, respectively.

$$\Delta\theta = \frac{\sqrt{\Delta^2 \hat{X}}}{\left| (\partial \langle \hat{X} \rangle / \partial \eta) (\partial \eta / \partial \theta) \right|},$$

$$\eta = |r_{pgv}|^2 = \left| \frac{r_{pg} + r_{gv} e^{2ik_{gz}d}}{1 + r_{pg}r_{gv} e^{2ik_{gz}d}} \right|^2,$$

$$r_{nm} = \frac{k_{nz}\varepsilon_m - k_{mz}\varepsilon_n}{k_{nz}\varepsilon_m + k_{mz}\varepsilon_n},$$

$$k_{nz} = \frac{2\pi}{\lambda} \sqrt{\varepsilon_n - \varepsilon_p(\sin\theta)^2},$$

$$k_{mz} = \frac{2\pi}{\lambda} \sqrt{\varepsilon_m - \varepsilon_p(\sin\theta)^2}, \quad (12)$$

where $\Delta^2 \hat{X}$ and $\langle \hat{X} \rangle$ can be obtained from Eq. (11).

In Fig. 7, we show that the incident angle sensitivity $\Delta\theta$ changing with θ when given parameters $g = 0.7$, $\theta_\alpha = 0$, $\theta_\beta = \pi$ and $|\alpha| = |\beta| = 50000$. It can be found that $\Delta\theta$ is relatively small around $\theta = 43.6208^\circ$ and $\theta = 43.6407^\circ$ except for the SPR angle. It is worth noting that the incident angle sensitivity can break through $(6 \times 10^{-6})^\circ$ which shows more accurate compared with the rotation precision of 0.04° in the weak measurement of IF shifts [34].

Moreover, to show the effect of the coherence amplitude $|\alpha|$ and $|\beta|$ on the incident angle sensitivity, at

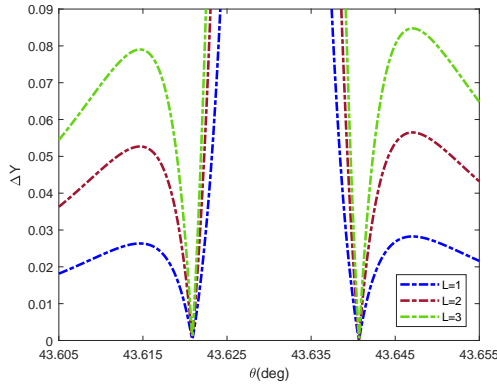


FIG. 6: (Color online) IF shifts sensitivity based on homodyne detection as a function of θ with $g = 0.7$, $\theta_\alpha = 0$, $\theta_\beta = \pi$, and $|\alpha| = |\beta| = 50000$ for different L . The blue-dashed line, the wine-red-dashed line and the green-dashed line correspond to $L = 1$, $L = 2$ and $L = 3$, respectively.

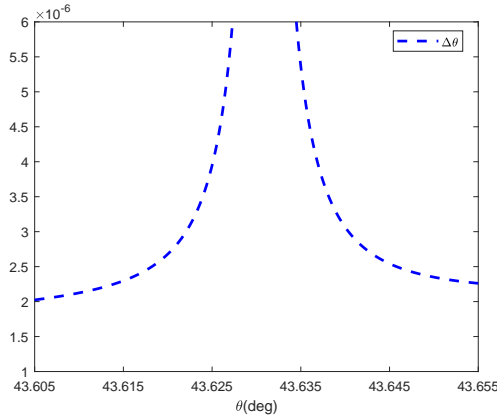


FIG. 7: (Color online) Incident angle sensitivity based on homodyne detection as a function of θ with $g = 0.7$, $\theta_\alpha = 0$, $\theta_\beta = \pi$, and $|\alpha| = |\beta| = 50000$.

$\theta = 43.6208^\circ$ and $\theta = 43.6407^\circ$, we also plot the incident angle sensitivity as a function of $|\alpha|$ and $|\beta|$ in Fig. 8(a) and 8(b), respectively. It can be found that, the incident angle sensitivity $\Delta\theta$ decreases sharply with the increase of $|\alpha|$ and $|\beta|$, for the case of $\theta = 43.6208^\circ$ and $\theta = 43.6407^\circ$.

VI. THE QCRB AND SNL OF IF SHIFTS AND INCIDENT ANGLE

As we all know, one can also obtain the precision limit of IF shifts and incident angle, respectively, without using any the detection method by calculating the QFI of the probe state, which characterizes the maximum amount

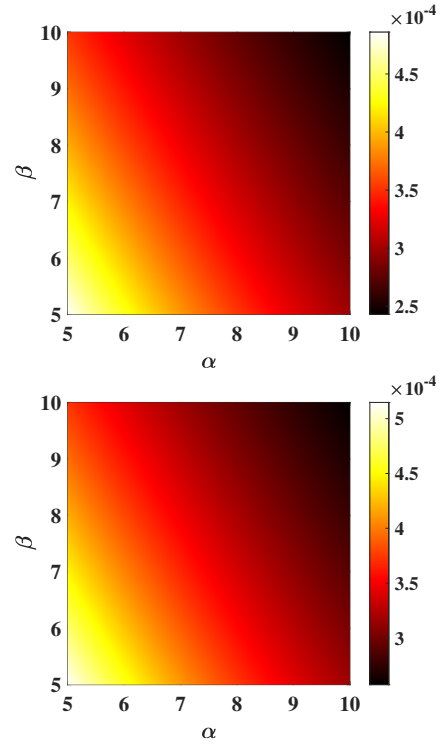


FIG. 8: (Color online) Incident angle sensitivity based on homodyne detection as a function of the coherent amplitude $|\alpha|$ and $|\beta|$ with $g = 0.7$, $\theta_\alpha = 0$, $\theta_\beta = \pi$ at (a) $\theta = 43.6208^\circ$, and (b) $\theta = 43.6407^\circ$, respectively.

of information about IF shifts and incident angle. Under lossless cases, for a pure quantum state, the QFI of IF shifts and incident angle can be respectively expressed as

$$\begin{aligned} F_Y &= 4[\langle \psi'_Y | \psi'_Y \rangle - |\langle \psi'_Y | \psi_Y \rangle|^2], \\ F_\theta &= 4[\langle \psi'_\theta | \psi'_\theta \rangle - |\langle \psi'_\theta | \psi_\theta \rangle|^2], \end{aligned} \quad (13)$$

where $|\psi_\Gamma\rangle = \hat{U}_{BS} \hat{S}(\xi_1) |\psi_{in}\rangle |0\rangle_{v_a}$, $\Gamma = Y, \theta$ is the state vector prior to the second OPA and $|\psi'_\Gamma\rangle = \partial |\psi_\Gamma\rangle / \partial \Gamma$. Then, for our scheme, the QFI of IF shifts and incident angle can be respectively given by

$$\begin{aligned} F_Y &= 4 \left[\langle \hat{H}_Y^2 \rangle - \langle \hat{H}_Y \rangle^2 \right] \\ &= \frac{(d\eta/dY)^2}{\eta(1-\eta)} \langle \hat{a}^\dagger \hat{a} \rangle, \\ F_\theta &= 4 \left[\langle \hat{H}_\theta^2 \rangle - \langle \hat{H}_\theta \rangle^2 \right] \\ &= \frac{(d\eta/d\theta)^2}{\eta(1-\eta)} \langle \hat{a}^\dagger \hat{a} \rangle, \end{aligned} \quad (14)$$

where $\langle \cdot \rangle$ is the average value under the state $\hat{S}(\xi_1) |\alpha\rangle_a |\beta\rangle_b |0\rangle_{v_a}$ and

$$\begin{aligned}
\hat{H}_Y &= i(d\hat{U}_{BS}^\dagger/d\eta)(d\eta/dY)\hat{U}_{BS}, \\
\hat{H}_\theta &= i(d\hat{U}_{BS}^\dagger/d\eta)(d\eta/d\theta)\hat{U}_{BS}, \\
\langle \hat{a}^\dagger \hat{a} \rangle &= (|\alpha| \cosh g + |\beta| \sinh g)^2 + \sinh^2 g. \quad (15)
\end{aligned}$$

According to the Eq. (15), one can respectively get the QCRB ΔY_{QCRB} and $\Delta \theta_{QCRB}$ of IF shifts and incident angle, which denotes the lower bound of the IF shifts sensitivity, i.e.,

$$\begin{aligned}
\Delta Y_{QCRB} &= \frac{1}{\sqrt{vF_Y}}, \\
\Delta \theta_{QCRB} &= \frac{1}{\sqrt{vF_\theta}}, \quad (16)
\end{aligned}$$

where v is the number of trials and we set $v = 1$ for simplicity. We can clearly see from Eq. (17) that the larger the value of F_Y , the higher the IF shifts and incident angle sensitivity. The corresponding SNL of IF shifts and incident angle can be respectively derived as

$$\begin{aligned}
\Delta Y_{SNL} &= \frac{1}{\sqrt{(d\eta/dY)^2 \langle \hat{N} \rangle / 4\eta(1-\eta)}}, \\
\Delta \theta_{SNL} &= \frac{1}{\sqrt{(d\eta/d\theta)^2 \langle \hat{N} \rangle / 4\eta(1-\eta)}}, \quad (17)
\end{aligned}$$

where $\langle \hat{N} \rangle = (|\alpha|^2 + |\beta|^2) \cosh 2g + 2|\alpha||\beta| \sinh 2g + 2\sinh^2 g$ is the total mean photon number inside the SU(1,1) interferometer.

In order to see whether the precision of IF shifts can surpass the SNL, we make a comparison about IF shifts sensitivity, the SNL ΔY_{SNL} and the ΔY_{QCRB} , as shown in Fig. 9. The parameters here are the same as those in Fig. 4. It can be seen from Fig. 9 that IF shifts sensitivity (blue-dashed line) can break through SNL (red-solid line) and is always surpassed by the QCRB (red-solid line). However, ΔY gradually approaches to the ultimate IF shift precision limit ΔY_{QCRB} as the incident angle gets close to $\theta = 43.6208^\circ$ and $\theta = 43.6407^\circ$.

Moreover, to show the effects of the coherence amplitude $|\alpha|$ and $|\beta|$ on the QCRB, we also plot the ΔY_{QCRB} as a function of $|\alpha|$ and $|\beta|$ at $\theta = 43.6208^\circ$ and $\theta = 43.6407^\circ$ in Figs. 10(a) and 10(b). It can be seen that the value of ΔY_{QCRB} decreases with the increase of $|\alpha|$ and $|\beta|$.

Further, we also illustrate the incident angle sensitivity $\Delta \theta$, the SNL $\Delta \theta_{SNL}$ and the QCRB $\Delta \theta_{QCRB}$ as a function of the incident angle θ in Fig. 11. The parameters here are the same as those in Fig. 7. It can be seen from Fig. 11 that the incident angle sensitivity (blue-dashed line) can also beat the SNL (green-dashed line), but can not break through the QCRB (black-dashed line).

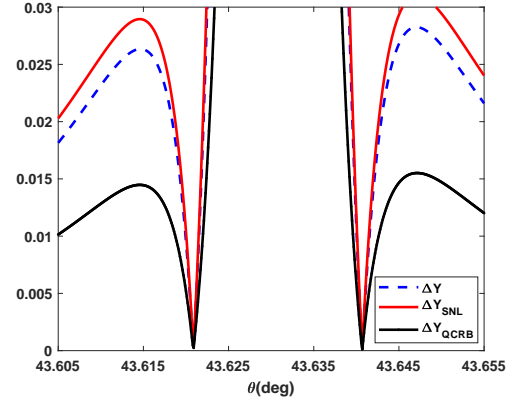


FIG. 9: (Color online) ΔY , ΔY_{QCRB} and ΔY_{SNL} as a function of incident angle θ with $g = 0.7$, $\theta_\alpha = 0$, $\theta_\beta = \pi$ and $L = 1$, respectively.

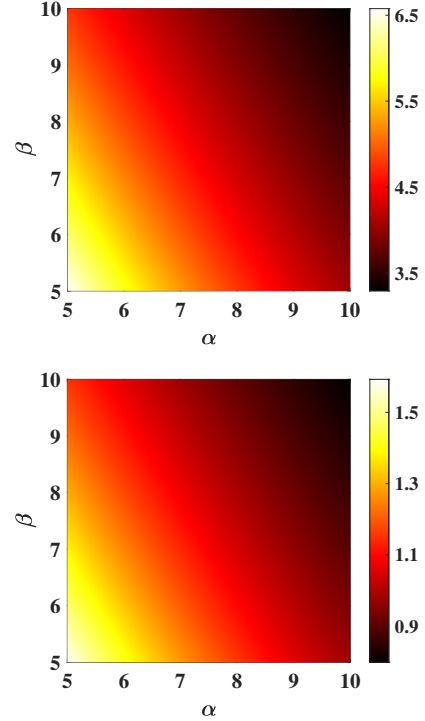


FIG. 10: (Color online) The ΔY_{QCRB} as a function of the coherent amplitude $|\alpha|$ and $|\beta|$ with $g = 0.7$, $\theta_\alpha = 0$, $\theta_\beta = \pi$ and $L = 1$ at (a) $\theta = 43.6208^\circ$, and (b) $\theta = 43.6407^\circ$, respectively.

VII. CONCLUSIONS

In conclusion, we presented a theoretical estimation scheme of the IF shift and incident angle based on the Kretschmann structure which is placed in an SU(1,1) interferometer. Then, we respectively derived the sensitivity of IF shifts and incident angle via the homodyne

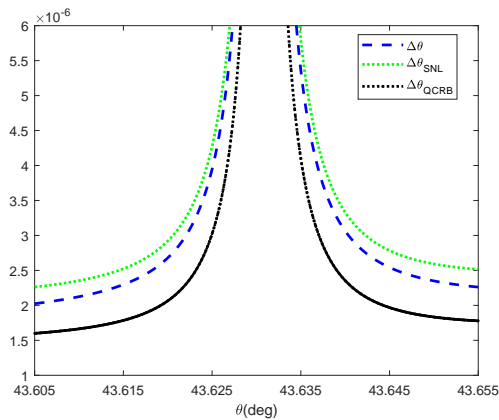


FIG. 11: (Color online) $\Delta\theta$, $\Delta\theta_{QCRB}$ and $\Delta\theta_{SNL}$ as a function of incident angle θ with $g = 0.7$, $\theta_\alpha = 0$, $\theta_\beta = \pi$, respectively.

detection. Our analysis shows that, at the incident angle $\theta = 43.6208^\circ$ and $\theta = 43.6407^\circ$, the maximal IF shifts and

the minimum IF shifts sensitivity can be obtained simultaneously. Moreover, we find that the quanta number of the orbit angular momentum is unfavorable for improving the IF shift sensitivity. Actually, the sensitivity of IF shifts can be obtained by the weak measurement scheme. Therefore, we also investigated the incident angle sensitivity in our scheme. The numerical results showed that the incident angle sensitivity can break through $(6 \times 10^{-6})^\circ$ which shows more accurate compared with the rotation precision of 0.04° in the weak measurement of IF shifts [39]. More importantly, both the sensitivity of IF shifts and incident angle can beat the SNL, even approaching the QCRB at the incident angle $\theta = 43.6208^\circ$ and $\theta = 43.6407^\circ$. Finally, we discussed the effects of the coherent amplitude on the IF shifts, incident angle sensitivity and QCRB. The results revealed that the increase of coherent amplitude is beneficial to improve the sensitivity of IF shifts and incident angle. Our work provided a novel scheme for measuring micro-displacement in SPR sensor, which has great application potential in the field of quantum sensor and quantum information processing.

-
- [1] R. Demkowicz-Dobrzański and L. Maccone, “Using Entanglement Against Noise in Quantum Metrology,” *Phys. Rev. Lett.* 113(25), 250801 (2014).
- [2] L. Pezzé and A. Smerzi, “Mach-Zehnder Interferometry at the Heisenberg Limit with Coherent and Squeezed-Vacuum Light,” *Phys. Rev. Lett.* 100(7), 073601 (2008).
- [3] V. Giovannetti, S. Lloyd, and L. Maccone, “Quantum metrology,” *Phys. Rev. Lett.* 96(1), 010401 (2006).
- [4] R. Demkowicz-Dobrzański, M. Jarzyna, and J. Kolodyński, “Quantum limits in optical interferometry,” *Prog. Optics.* 60, 345-435 (2015).
- [5] F. Hudelist, J. Kong, C. J. Liu, J. T. Jing, Z. Y. Ou, and W. P. Zhang, “Quantum metrology with parametric amplifier-based photon correlation interferometers,” *Nat. Commun.* 5(1), 3049 (2014).
- [6] A. Datta, L. J. Zhang, N. Thomas-Peter, U. Dorner, B. J. Smith, and Ian A. Walmsley, “Quantum metrology with imperfect states and detectors,” *Phys. Rev. A* 83(6), 063836 (2011).
- [7] E. Oelker, L. Barsotti, S. Dwyer, D. Sigg, and N. Mavalvala, Squeezed light for advanced gravitational wave detectors and beyond, *Opt. Express* 22, 21106 (2014).
- [8] H. Vahlbruch, D. Wilken, M. Mehmet, and B. Willke, Laser Power Stabilization beyond the Shot Noise Limit Using Squeezed Light, *Phys. Rev. Lett.* 121, 173601 (2018).
- [9] M. Tsang, Quantum Imaging beyond the Diffraction Limit by Optical Centroid Measurements, *Phys. Rev. Lett.* 102, 253601 (2009).
- [10] N. Bornman, S. Prabhakar, A. Valles, J. Leach, and A. Forbes, Ghost imaging with engineered quantum states by Hong–Ou–Mandel interference, *New J. Phys.* 21, 073044 (2019).
- [11] S. D. Huver, C. F. Wildfeuer, J. P. Dowling, Entangled Fock states for robust quantum optical metrology, imaging, and sensing, *Phys. Rev. A* 78, 063828 (2008).
- [12] Boeyens, Julia, Stella Seah, and Stefan Nimmrichter. “Uninformed Bayesian quantum thermometry.” *Phys. Rev. A* 104.5 (2021): 052214.
- [13] Alves, Gabriel O., and Gabriel T. Landi. “Bayesian estimation for collisional thermometry.” *Phys. Rev. A* 105.1 (2022): 012212.
- [14] Jørgensen, Mathias R., et al. “Bayesian quantum thermometry based on thermodynamic length.” *Physical Review A* 105.4 (2022): 042601.
- [15] A. A. Michelson and E. W. Morley, “On the relative motion of the earth and of the luminiferous ether,” *Am. J. Sci.* 34, 333–345 (1887).
- [16] M. O. Scully and M. S. Zubairy, *Quantum Optics* (Cambridge University, 1997).
- [17] H. Lee, P. Kok, and J. P. Dowling, “A quantum Rosetta stone for interferometry,” *J. Mod. Opt.* 49, 2325–2338 (2002).
- [18] C. M. Caves, “Quantum-mechanical noise in an interferometer,” *Phys. Rev. D* 23, 1693–1708 (1981).
- [19] M. Xiao, L. A. Wu, and H. J. Kimble, “Precision measurement beyond the shot-noise limit,” *Phys. Rev. Lett.* 59, 278–281 (1987).
- [20] B. Yurke, S. L. McCall, and J. R. Klauder, “SU(2) and SU(1,1) interferometers,” *Phys. Rev. A* 33, 4033–4054 (1986).
- [21] D. Li, C.-H. Yuan, Z. Y. Ou, and W. Zhang, The phase sensitivity of an SU(1,1) interferometer with coherent and squeezed-vacuum light, *New J. Phys.* 16, 073020 (2014).
- [22] D. Li, B. T. Gard, Y. Gao, C.-H. Yuan, W. Zhang, H. Lee, and J. P. Dowling, Phase sensitivity at the Heisenberg limit in an SU(1,1) interferometer via parity detection, *Phys. Rev. A* 94, 063840 (2016).
- [23] Zheng, K., Mi, M., Wang, B., Xu, L., Hu, L., Liu, S., ... & Zhang, L. (2020). Quantum-enhanced stochastic phase estimation with the SU(1, 1) interferometer. *Photonics Research*, 8(10), 1653-1661.
- [24] Chang, S., Ye, W., Zhang, H., Hu, L., Huang, J., & Liu,

- S. (2022). Improvement of phase sensitivity in an SU(1, 1) interferometer via a phase shift induced by a Kerr medium. *Physical Review A*, 105(3), 033704.
- [25] Q.-K. Gong, D. Li, C.-H. Yuan, Z.-Y. Qu, and W.-P. Zhang, Phase estimation of phase shifts in two arms for an SU(1,1) interferometer with coherent and squeezed vacuum states, *Chin. Phys. B* 26, 94205 (2017).
- [26] X. Ling, X. Zhou, K. Huang, Y. Liu, C.W. Qiu, H. Luo, S. Wen, *Rep. Progr. Phys.* 80 (2017) 066401.
- [27] Tan X., Zhu X. *Opt. Lett.*, 41 (2016), pp. 2478-2481.
- [28] Yin X., Ye Z., Rho J., Wang Y., Zhang X. *Science*, 339 (2013), p. 1405
- [29] Zhu W., Yu J., Guan H., Lu H., Tang J., Luo Y., Chen Z. *Opt. Express*, 25 (2017), p. 5196
- [30] Zhou X., Ling X., Luo H., Wen S. *Appl. Phys. Lett.*, 101 (2012), p. 1530
- [31] Caves, Carlton M. "Quantum-mechanical radiation-pressure fluctuations in an interferometer." *Physical Review Letters* 45.2 (1980): 75.
- [32] Giovannetti, Vittorio, Seth Lloyd, and Lorenzo Maccone. "Quantum metrology." *Physical review letters* 96.1 (2006): 010401.
- [33] Z. Y. Ou, "Enhancement of the phase-measurement sensitivity beyond the standard quantum limit by a nonlinear interferometer," *Phys. Rev. A* 85, 023815 (2012).
- [34] Prajapati, C., & Viswanathan, N. K. (2017). Simultaneous weak measurement of angular and spatial Goos-Hänchen and Imbert-Fedorov shifts. *Journal of Optics*, 19(10), 105611.
- [35] Guo, Xinyi, et al. "Surface plasmon resonance enhanced Goos-Hänchen and Imbert-Fedorov shifts of Laguerre-Gaussian beams." *Optics Communications* 445 (2019): 5-9.
- [36] Wang, Hailong, et al. "Nonlinear interferometric surface-plasmon-resonance sensor." *Optics Express* 29.7 (2021): 11194-11206.
- [37] W. N. Plick, J. P. Dowling, G. S. Agarwal, Coherent-light boosted, sub-shot noise, quantum interferometry, *New J. Phys.* 12, 083014 (2010).
- [38] L. L. Guo, Y. F. Yu, Z. M. Zhang, Improving the phase sensitivity of an SU(1,1) interferometer with photon-added squeezed vacuum light, *Opt. Express* 26, 29099 (2018).
- [39] S. Ataman, Phase sensitivity of a Mach-Zehnder interferometer with single-intensity and difference-intensity detection, *Phys. Rev. A* 98, 043856 (2018).
- [40] P. M. Anisimov, G. M. Raterman, A. Chiruvelli, W. N. Plick, S. D. Huver, H. Lee, and J. P. Dowling, Quantum Metrology with Two-Mode Squeezed Vacuum: Parity Detection Beats the Heisenberg Limit, *Phys. Rev. Lett.* 104, 103602 (2010).
- [41] D. Li, B. T. Gard, Y. Gao, C. H. Yuan, W. P. Zhang, H. Lee, J. P. Dowling, Phase sensitivity at the Heisenberg limit in an SU(1,1) interferometer via parity detection, *Phys. Rev. A* 94, 063840 (2016).
- [42] S. Adhikari, N. Bhusal, C. You, H. Lee, and J. P. Dowling, Phase estimation in an SU(1,1) interferometer with displaced squeezed states, *Opt. Express* 1, 438 (2018).
- [43] Wang, H., Fu, Z., Ni, Z., Zhang, X., Zhao, C., Jin, S., & Jing, J. (2021). Nonlinear interferometric surface-plasmon-resonance sensor. *Optics Express*, 29(7), 11194-11206.